Computers and Mathematics with Applications 74 (2017) 948–961

Contents lists available at ScienceDirect

Computers and Mathematics with Applications

journal homepage: www.elsevier.com/locate/camwa

Numerical analysis of a first-order in time implicit-symplectic scheme for predator–prey systems

Fasma Diele [a,*], Marcus Garvie [b], Catalin Trenchea [c]

[a] Istituto per le Applicazioni del Calcolo M. Picone, CNR, Via Amendola 122, 70126 Bari, Italy
[b] Department of Mathematics and Statistics, University of Guelph, Guelph, ON, Canada N1G 2W1
[c] Department of Mathematics, 301 Thackeray Hall, University of Pittsburgh, Pittsburgh, PA 15260, United States

ARTICLE INFO

Article history:
Available online 24 May 2017

Keywords:
Reaction–diffusion predator–prey systems
Semi-discrete in time formulation
Numerical schemes

ABSTRACT

The numerical solution of reaction–diffusion systems modelling predator–prey dynamics using implicit-symplectic (IMSP) schemes is relatively new. When applied to problems with chaotic dynamics they perform well, both in terms of computational effort and accuracy. However, until the current paper, a rigorous numerical analysis was lacking. We analyse the semi-discrete in time approximations of a first-order IMSP scheme applied to spatially extended predator–prey systems. We rigorously establish semi-discrete *a priori* bounds that guarantee positive and stable solutions, and prove an optimal *a priori* error estimate. This analysis is an improvement on previous theoretical results using standard implicit–explicit (IMEX) schemes. The theoretical results are illustrated via numerical experiments in one and two space dimensions using fully-discrete finite element approximations.

1. Introduction

In spatial ecology the deterministic description of population densities that are continuous in space and time are modelled by reaction–diffusion systems, which can be analysed by means of the well-developed theories of differential equations and dynamical systems [1]. We focus on spatially-extended predator–prey models described by reaction–diffusion systems in the following general form

$$\frac{\partial u}{\partial t} = f(u, v) + D_u \Delta u, \tag{1.1a}$$

$$\frac{\partial v}{\partial t} = g(u, v) + D_v \Delta v, \tag{1.1b}$$

where $u(x, t)$ and $v(x, t)$ represent population densities of prey and predators at time t and position x and D_u and D_v are positive constant diffusion coefficients. The equations evolve in $\Omega_T := \Omega \times (0, T)$ where the domain Ω is a bounded and open subset of $\mathbb{R}^d$, $d \leq 3$. The boundary of the domain $\partial\Omega$ is assumed to belong to the class of C^1. The system is augmented with initial conditions

$$u_0(x) := u(x, 0), \qquad v_0(x) := v(x, 0), \quad x \in \Omega, \tag{1.1c}$$

* Corresponding author.
E-mail addresses: f.diele@ba.iac.cnr.it (F. Diele), mgarvie@uoguelph.ca (M. Garvie), trenchea@pitt.edu (C. Trenchea).

http://dx.doi.org/10.1016/j.camwa.2017.04.030
0898-1221/

and the homogeneous Neumann boundary conditions

$$\frac{\partial u}{\partial \nu} = \frac{\partial v}{\partial \nu} = 0 \quad \text{on } \partial\Omega \times (0, T). \tag{1.1d}$$

In the above equations ν denotes the outward unit normal to $\partial\Omega$ and Δ denotes the Laplacian operator $\sum_{i=1}^{d} \frac{\partial^2}{\partial x_i^2}$.

Results from semigroup theory and an *a priori* estimate were used in Garvie and Trenchea [2] to prove the global existence and uniqueness of the classical solutions of the predator–prey system (1.1a)–(1.1d) on two specific systems. For the well-posedness of the problem, we assume the nonlinearities f, g are globally Lipschitz, i.e., there exists $L > 0$ such that

$$|f(u_1, v_1) - f(u_2, v_2)| + |g(u_1, v_1) - g(u_2, v_2)| \le L(|u_1 - u_2| + |v_1 - v_2|), \tag{1.2}$$

for all u_i and v_i in a compact subset of $\mathbb{R}^+ \times \mathbb{R}^+$ and, in order to assure the non-negativity of solutions corresponding to biologically meaningful densities, the reaction kinetics satisfy

$$f(0, v), g(u, 0) \ge 0, \quad \forall u, v \ge 0. \tag{1.3}$$

Consequently, if the initial data $(u_0(x), v_0(x))$ is chosen in $[0, +\infty)^2$ for all $x \in \Omega$, then by a maximum principle the solution $(u(x, t), v(x, t))$ also lies in $[0, +\infty)^2$, which is a positively invariant region for the system.

Moreover, we assume that $f(u, v)$ has *logistic* dominated growth in the first variable, namely

$$f(u, v) \le u(1 - u), \quad \forall u, v \ge 0, \tag{1.4}$$

and the function g satisfies a sub-linear growth in the second variable, i.e., there exists $C_g > 0$ such that

$$g(u, v) \le C_g v, \quad \forall u, v \ge 0. \tag{1.5}$$

Notice that from the assumptions (1.3)–(1.5) it is easy to show that for all $u, v \ge 0$

$$g(u, 0) = f(0, v) = 0. \tag{1.6}$$

The assumptions (1.3)–(1.5) are not overly restrictive as the principal population dynamics models, based on logistic prey growth and 'Holling type' functional response of the predators, satisfy these conditions [3–5]. This is the case of models that couple logistic prey growth with Holling II and IV functional predator responses [6] as well as the well-known Rosenzweig–MacArthur model [7].

The reaction–diffusion system (1.1a)–(1.1d) includes a class of predator–prey models exhibiting instabilities [8]. Reaction–diffusion systems with logistic prey growth and 'Holling type' functional response of the predators exhibit spiral waves, target waves, and spatiotemporal chaos. However, diffusion induced instability is not possible for systems of this type. Numerical schemes used to approximate such dynamics should be sufficiently robust to reproduce the correct behaviour of the continuous solutions. Stability, high-order consistency and preservation of geometric properties form three pillars on which numerical methods for differential equations rest [9]. The need for a rigorous error analysis of the numerical schemes to approximate the reaction–diffusion dynamics was highlighted in the papers by M. Garvie, C. Trenchea and their co-authors in [10,2,11]. In particular, two implicit–explicit schemes (IMEX) have been extensively analysed by the authors in Garvie and Trenchea [10] using the standard Galerkin finite element method with piecewise linear continuous basis functions.

The preservation of properties of the exact flow under numerical discretization is a more recent field of research. For an exhaustive study of geometric integrators, especially for ordinary differential systems, we refer to the monograph by Hairer et al. [12]. Recently, attention has been devoted to the geometric integration of reaction–diffusion equations. For example, splitting methods were introduced by Hansen et al. [9] to preserve positivity of the numerical approximations.

Implicit-symplectic (IMSP) schemes are numerical integrators based on an implicit scheme for the stiff diffusive term and a geometric integrator for the reaction function. In Diele et al. [13,14] IMSP schemes were proposed as novel numerical schemes for the simulation of population and metapopulation predator–prey dynamics. Symplectic partitioned Runge–Kutta schemes based on composition of Symplectic Euler steps were implemented for approximating Lotka–Volterra (LV) reaction–diffusion dynamics. The authors were motivated by the classical results for the local Poisson nature of the LV dynamics (see, for example, Hairer et al. [12]). Poisson integrators (for example, Symplectic Euler method and composition of symplectic Euler steps) reproduce the correct qualitative behaviour of the theoretical solution and achieve an accurate long-time numerical approximation [12,15]. A stability analysis of IMSP schemes in terms of the diffusion and the reaction time-scales was recently developed in Settanni and Sgura [16]. Their numerical simulations reveal that IMSP schemes provide the best choice for spatio-temporal dynamics of standing oscillations around an equilibrium of centre type (see e.g. Guckenheimer and Holmes [17]).

In this paper we undertake the rigorous numerical analysis of the semi-discrete in time approximations of a first-order IMSP scheme applied to the spatially extended predator–prey system (1.1a)–(1.1d). In Diele et al. [13,14] the method of lines was used. Here, we consider a more technical methodology based on the analysis of a semi-discrete in time formulation of the scheme. We do not undertake the numerical analysis of the fully-discrete problems, however, the analysis of the semi-discrete problems provides the basis on which such a task could be carried out. A novel aspect of the current work is the use of the IMSP approach in conjunction with the standard Galerkin finite element method to solve reaction–diffusion systems.

The remainder of this paper is organized as follows. In Section 2 we present the semi-discrete in time IMSP scheme for approximating system (1.1a)–(1.1d), and give conditions for positive and stable solutions together with an *a priori* error estimate. In Section 3 the fully discrete scheme is presented, and in Section 4 we give the results of some numerical experiments. Concluding comments are given in Section 5.

2. The semi-discrete in time IMSP approximation

2.1. Mathematical preliminaries

We introduce some mathematical notation and preliminaries. Consider the Banach space $L^2(\Omega)$ with norm

$$\|u\| := \left(\int_\Omega |u(x)|^2 dx\right)^{1/2},$$

where $(\cdot,\cdot)$ is the usual L^2 inner product. We let $\langle\cdot,\cdot\rangle$ denote the duality pairing between $(H^1(\Omega))'$ and $H^1(\Omega)$, where standard notation for the Sobolev space $H^1(\Omega)$ and its dual $(H^1(\Omega))'$ have been used. The norm of $(H^1(\Omega))'$ is denoted by $\|\cdot\|_*$. We also define $L^2(\Omega_T)$ as the Banach space $L^2(0,T,L^2(\Omega))$ of all the functions $u : (0,T) \to L^2(\Omega)$ such that $t \to \|u(t)\|$ is in $L^2(0,T)$, with norm

$$\|u\|_{L^2(\Omega_T)} := \left(\int_0^T \|u(t)\|^2 dt\right)^{1/2}.$$

A similar definition is used to denote the space $L^2(0,T,(H^1(\Omega))')$, the space of all the functions $u : (0,T) \to (H^1(\Omega))'$ such that $t \to \|u(t)\|_*$ is in $L^2(0,T)$ with norm

$$\|u\|_{L^2(0,T,(H^1(\Omega))')} := \left(\int_0^T \|u(t)\|_*^2 dt\right)^{1/2}.$$

With this notation the system (1.1a)–(1.1d) can be written in the following continuous in time weak formulation:
Find $u(\cdot,t), v(\cdot,t) \in H^1(\Omega)$ such that $(u(\cdot,0), v(\cdot,0)) = (u_0(\cdot), v_0(\cdot))$ and

$$\langle u_t, \chi\rangle + D_u(\nabla u, \nabla\chi) = \langle f(u,v), \chi\rangle, \tag{2.7a}$$

$$\langle v_t, \chi\rangle + D_v(\nabla v, \nabla\chi) = \langle g(u,v), \chi\rangle, \tag{2.7b}$$

for all $\chi \in H^1(\Omega)$ and for almost every $t \in (0,T)$.

2.2. The algorithm

We discretize the temporal horizon $(0,T)$ using a uniform mesh grid of $N+1$ points $t_n = n\Delta t, n = 0,\dots,N$, with constant time step $\Delta t = T/N$. Let the initial densities of predators and prey be $v_0(x)$ and $u_0(x)$ respectively, for all $x \in \Omega$. We define the first-order IMSP scheme (in weak form) as follows:
For $n = 0,\dots,N-1$ find $v^{n_1}, v^{n+1}, u^{n+1} \in H^1(\Omega)$ such that $(u^0, v^0) = (u_0(\cdot), v_0(\cdot))$ and for all $\chi \in H^1(\Omega)$

$$\left(\frac{u^{n+1}-u^n}{\Delta t}, \chi\right) + D_u(\nabla u^{n+1}, \nabla\chi) = (f(u^n, v^{n_1}), \chi), \tag{2.8a}$$

$$\left(\frac{v^{n+1}-v^n}{\Delta t}, \chi\right) + D_v(\nabla v^{n+1}, \nabla\chi) = (g(u^n, v^{n_1}), \chi), \tag{2.8b}$$

$$\left(\frac{v^{n_1}-v^n}{\Delta t}, \chi\right) = \left(g(u^n, v^{n_1}), \chi\right), \tag{2.8c}$$

or, equivalently:
For $n = 0,\dots,N-1$ find $v^{n_1}, u^{n_1}, v^{n+1}, u^{n+1} \in H^1(\Omega)$ such that $(u^0, v^0) = (u_0(\cdot), v_0(\cdot))$ and for all $\chi \in H^1(\Omega)$

$$\left(\frac{u^{n+1}-u^{n_1}}{\Delta t}, \chi\right) + D_u(\nabla u^{n+1}, \nabla\chi) = 0, \tag{2.9a}$$

$$\left(\frac{v^{n+1}-v^{n_1}}{\Delta t}, \chi\right) + D_v(\nabla v^{n+1}, \nabla\chi) = 0, \tag{2.9b}$$

$$\left(\frac{u^{n_1}-u^n}{\Delta t}, \chi\right) = \left(f(u^n, v^{n_1}), \chi\right), \tag{2.9c}$$

$$\left(\frac{v^{n_1}-v^n}{\Delta t}, \chi\right) = \left(g(u^n, v^{n_1}), \chi\right). \tag{2.9d}$$

From the formulation of the first order IMSP scheme (2.9a)–(2.9d), we see that it differs from the corresponding IMEX scheme only in the explicit discretization for v in (2.9c) and (2.9d) (the IMEX scheme evaluates f and g at (u^n, v^n)). Consequently, in the general case the IMSP scheme requires extra computational cost. However, whenever g depends at most linearly on v, the scheme (2.9c) and (2.9d) can be solved explicitly. This point will be clarified in Section 3.

In the following section we will use both (2.8a)–(2.8c) and (2.9a)–(2.9d) in order to prove positivity, stability and provide errors estimates.

2.3. Positivity

In the following theorem we give a bound on the time step which guarantees the positivity of IMSP solutions.

Theorem 2.1. *Assume the time step $\Delta t < 1/L$ and Ω is a domain of class C^1. Provided that the initial conditions are positive, i.e., $u_0(x) = u(x, 0) > 0$, $v_0(x) = v(x, 0) > 0$, for all $x \in \Omega$, then the solutions $u^n(x)$, $v^n(x)$ of the first-order scheme (2.9a)–(2.9d) are positive for all $n \geq 0$.*

Proof. We use an induction argument. Suppose that $u^n, v^n > 0$ in Ω, for a fixed arbitrary $n \geq 0$. First we prove that $v^{n_1}(x) \neq 0$ for all x in Ω. Assume, by contradiction, that there exists $x_\circ \in \Omega$ such that $v^{n_1}(x_\circ) = 0$. From (2.9d), using (1.6), we have that

$$0 = v^{n_1}(x_\circ) = v^n(x_\circ) + \Delta t g(u^n(x_\circ),\ v^{n_1}(x_\circ)) = v^n(x_\circ) > 0,$$

which is a contradiction. Moreover, from (2.9d), using (1.6), (1.2), and the assumption on the time step $\Delta t < 1/L$, we also have

$$|v^{n_1} - v^n| = \Delta t |g(u^n, v^{n_1}) - g(u^n, 0)| \leq \Delta t L |v^{n_1}| < |v^{n_1}|.$$

From the above relation, and the induction assumption $v^n(x) > 0$, it follows that $v^{n_1}(x) > 0$, for all x in Ω. From (2.9b) we therefore obtain

$$v^{n+1} - \Delta t D_v \Delta v^{n+1} = v^{n_1} > 0 \quad \text{in } \Omega.$$

Finally, the strong maximum principle and Hopf's lemma for elliptic equations (see, e.g., Barbu [18], Evans [19], DiBenedetto [20]) yield the positivity of v^{n+1}. In a similar way it is easy to prove that u^{n_1} in (2.9c) and, consequently, u^{n+1} in (2.9a) are both positive. ■

2.4. Stability

In this section we prove an *a priori* estimate for the semi-discrete solutions (2.8a)–(2.8c) depending on the initial data. First define

$$\Delta t_s := 1/\max\{1, 2C_g\}. \tag{2.10}$$

Theorem 2.2. *Assume the time step satisfies $\Delta t \leq \Delta t_s$. Then the solution to (2.8a)–(2.8c) satisfies the following energy estimate:*

$$\begin{aligned} &\|u^N\|^2 + \|v^N\|^2 + \sum_{n=0}^{N-1} \left(\|u^{n+1} - u^n\|^2 + \frac{1}{2}\|v^{n+1} - v^n\|^2 \right) + \Delta t \sum_{n=0}^{N-1} \left(2D_u \|\nabla u^{n+1}\|^2 + D_v \|\nabla v^{n+1}\|^2 \right) \\ &\quad \leq \exp\left(\frac{2\Delta t N}{\Delta t_s - \Delta t} \right) \left(\|u_0\|^2 + \|v_0\|^2 \right). \end{aligned} \tag{2.11}$$

Proof. First we derive an energy estimate for u^n. We take $\chi = u^{n+1}$ in (2.8a), and use the Cauchy–Schwarz inequality, (1.4) and the positivity of u^{n+1} to obtain

$$\begin{aligned} &\frac{1}{2\Delta t} \left(\|u^{n+1}\|^2 - \|u^n\|^2 + \|u^{n+1} - u^n\|^2 \right) + D_u \|\nabla u^{n+1}\|^2 = \left(f(u^n, v^{n_1}), u^{n+1} \right) \\ &\quad \leq \int_\Omega \left(u^n u^{n+1} - (u^n)^2 u^{n+1} \right) d\Omega \leq \frac{1}{2}\|u^{n+1}\|^2 + \frac{1}{2}\|u^n\|^2. \end{aligned}$$

The discrete Grönwall inequality (see e.g. [21,22, Lemma 5.1.1]) yields

$$\|u^N\|^2 + \frac{1}{1 - \Delta t} \sum_{n=0}^{N-1} \|u^{n+1} - u^n\|^2 + \frac{2\Delta t}{1 - \Delta t} D_u \sum_{n=0}^{N-1} \|\nabla u^{n+1}\|^2 \leq \|u_0\|^2 \exp\left(\frac{2\Delta t N}{1 - \Delta t} \right), \quad \forall \Delta t \leq 1. \tag{2.12}$$

To obtain an energy estimate for v^n, we take $\chi = v^{n_1}$ in (2.8c), and use assumptions (2.10), (1.5) to obtain

$$\frac{1}{2\Delta t}\left(\|v^{n_1}\|^2 - \|v^n\|^2 + \|v^{n_1} - v^n\|^2\right) = \langle g(u^n, v^{n_1}), v^{n_1}\rangle \le C_g\|v^{n_1}\|^2,$$

which yields

$$\|v^{n_1}\|^2 + \frac{1}{1 - 2\Delta t C_g}\|v^{n_1} - v^n\|^2 \le \frac{1}{1 - 2\Delta t C_g}\|v^n\|^2. \tag{2.13}$$

Similarly, let $\chi = v^{n+1}$ in (2.8b), use (2.13), sum for $n = 0, \ldots, N-1$, and apply the discrete Grönwall inequality to get

$$\|v^N\|^2 + \frac{1}{1 - \Delta t C_g}\sum_{n=0}^{N-1}\|v^{n+1} - v^n\|^2 + \frac{2\Delta t D_v}{1 - \Delta t C_g}\sum_{n=0}^{N-1}\|\nabla v^{n+1}\|^2 \le \|v_0\|^2 \exp\left(\frac{2N\Delta t C_g}{1 - 2\Delta t C_g}\right), \quad \forall \Delta t \le \frac{1}{2C_g}. \tag{2.14}$$

Finally (2.12) and (2.14) imply (2.11). ■

2.5. Error analysis

Let $\varepsilon_u^n, \varepsilon_v^n \in (H^1(\Omega))'$ denote the following local truncation errors for scheme (2.8a)–(2.8c), satisfying

$$\langle \varepsilon_u^n, \chi\rangle := \frac{1}{\Delta t}\langle u(t_n) - u(t_{n-1}), \chi\rangle - \langle f(u(t_{n-1}), v(t_n)), \chi\rangle + D_u(\nabla u(t_n), \nabla\chi),$$
$$\langle \varepsilon_v^n, \chi\rangle := \frac{1}{\Delta t}\langle v(t_n) - v(t_{n-1}), \chi\rangle - \langle g(u(t_{n-1}), v(t_n)), \chi\rangle + D_v(\nabla v(t_n), \nabla\chi),$$

where $\chi \in H^1(\Omega)$. Furthermore, let $e_u^n, e_v^n \in H^1(\Omega)$ denote the point-wise errors

$$e_u^n = u(t_n) - u^n, \qquad e_v^n = v(t_n) - v^n,$$

satisfying the following equations:

$$\frac{e_u^{n+1} - e_u^n}{\Delta t} - D_u\Delta_h e_u^{n+1} = f(u(t_n), v(t_{n+1})) - f(u^n, v^{n_1}) + \varepsilon_u^{n+1}, \tag{2.15a}$$
$$\frac{e_v^{n+1} - e_v^n}{\Delta t} - D_v\Delta_h e_v^{n+1} = g(u(t_n), v(t_{n+1})) - g(u^n, v^{n_1}) + \varepsilon_v^{n+1}, \tag{2.15b}$$

where Δ_h is a discrete linear operator approximating the continuous Laplacian.

Lemma 2.1. *Assume the classical solution of (1.1a)–(1.1d) has the following regularity:*

$$\frac{du}{dt}, \frac{dv}{dt}, \frac{d^2u}{dt^2}, \frac{d^2v}{dt^2} \in L^2(0, T, (H^1(\Omega))'). \tag{2.16}$$

Then the truncation error satisfies the following bound:

$$\left[\Delta t\sum_{n=0}^{N-1}\left(\frac{1}{D_u}\|\varepsilon_u^{n+1}\|_*^2 + \frac{1}{D_v}\|\varepsilon_v^{n+1}\|_*^2\right)\right]^{\frac{1}{2}}$$
$$\le \Delta t\left[\int_{t_0}^{t_N}\frac{1}{D_u}\left(\left\|\frac{d^2u}{dt^2}(t)\right\|_* + L\left\|\frac{du}{dt}(t)\right\|_*\right)^2 + \frac{1}{D_v}\left(\left\|\frac{d^2v}{dt^2}(t)\right\|_* + L\left\|\frac{dv}{dt}(t)\right\|_*\right)^2 dt\right]^{\frac{1}{2}}. \tag{2.17}$$

Proof. Using the Taylor expansion to first-order

$$u(t_n) = u(t_{n+1}) - \Delta t\frac{du}{dt}(t_{n+1}) + \int_{t_n}^{t_{n+1}}(t - t_n)\frac{d^2u}{dt^2}(t)dt,$$

and the continuous in time equations (2.7a)–(2.7b), yields

$$\langle \varepsilon_u^{n+1}, \chi\rangle = -\left\langle\frac{1}{\Delta t}\int_{t_n}^{t_{n+1}}(t - t_n)\frac{d^2u}{dt^2}(t)dt, \chi\right\rangle + \left(f(u(t_{n+1}), v(t_{n+1})) - f(u(t_n), v(t_{n+1})), \chi\right),$$
$$\langle \varepsilon_v^{n+1}, \chi\rangle := -\left\langle\frac{1}{\Delta t}\int_{t_n}^{t_{n+1}}(t - t_n)\frac{d^2v}{dt^2}(t)dt, \chi\right\rangle + \left(g(u(t_{n+1}), v(t_{n+1})) - g(u(t_n), v(t_{n+1})), \chi\right).$$

Using the Lipschitz assumption (1.2) and Taylor expansion we have

$$\left|\left(f(u(t_{n+1}),v(t_{n+1}))-f(u(t_n),v(t_{n+1})),\chi\right)\right| \le L\int_{t_n}^{t_{n+1}}\left\|\frac{du}{dt}(t)\right\|_*dt\|\chi\|_1,$$
$$\left|\left(g(u(t_{n+1}),v(t_{n+1}))-g(u(t_n),v(t_{n+1})),\chi\right)\right| \le L\int_{t_n}^{t_{n+1}}\left\|\frac{dv}{dt}(t)\right\|_*dt\|\chi\|_1,$$

and therefore

$$\|\varepsilon_u^{n+1}\|_* \le \int_{t_n}^{t_{n+1}}\left(\left\|\frac{d^2u}{dt^2}(t)\right\|_* + L\left\|\frac{du}{dt}(t)\right\|_*\right)dt,$$
$$\|\varepsilon_v^{n+1}\|_* \le \int_{t_n}^{t_{n+1}}\left(\left\|\frac{d^2v}{dt^2}(t)\right\|_* + L\left\|\frac{dv}{dt}(t)\right\|_*\right)dt,$$

which yields (2.17). ■

Using (2.15a)–(2.15b) we establish an energy estimate for the local truncation errors.

Lemma 2.2. *Under assumption (1.2), for sufficiently small time steps*

$$\Delta t \le \Delta t_\circ := 1/\max\{D_u+7L, D_v+11L\},$$

the first-order symplectic scheme (2.8a)–(2.8c) satisfies the following estimate

$$\begin{aligned}
&\|e_u^N\|^2+\|e_v^N\|^2+\frac{\Delta t}{1-\Delta t/\Delta t_\circ}\sum_{n=0}^{N-1}\left(D_u\|\nabla e_u^{n+1}\|^2+D_v\|\nabla e_v^{n+1}\|^2\right)\\
&\le \frac{1}{1-\Delta t/\Delta t_\circ}\Bigg[(1+2\Delta tL-\Delta t/\Delta t_\circ)\left(\|e_u^0\|^2+\|e_v^0\|^2\right)\\
&\quad+\Delta t\sum_{n=0}^{N-1}\left(\frac{1}{D_u}\|\varepsilon_u^{n+1}\|_*^2+\frac{1}{D_v}\|\varepsilon_v^{n+1}\|_*^2\right)+4\Delta t^2L\left\|\frac{dv}{dt}\right\|^2_{L^2(0,T;L^2(\Omega))}\\
&\quad+2\Delta t^2LC_g\|v_0\|^2\exp\left(\frac{2N\Delta tC_g}{1-2\Delta tC_g}\right)\Bigg]\exp\left(\frac{N\Delta t}{\Delta t_\circ-\Delta t}\right).
\end{aligned}\tag{2.18}$$

Proof. We test equation (2.15a) with e_u^{n+1}, test equation (2.15b) with e_v^{n+1}, add, use the polarization identity

$$\frac{1}{2}(|a-b|^2-a^2-b^2)=-ab$$

and the Lipschitz assumption (1.2) yielding

$$\begin{aligned}
&\frac{1}{2\Delta t}\left(\|e_u^{n+1}\|^2-\|e_u^n\|^2+\|e_u^{n+1}-e_u^n\|^2\right)+\frac{1}{2\Delta t}\left(\|e_v^{n+1}\|^2-\|e_v^n\|^2+\|e_v^{n+1}-e_v^n\|^2\right)+D_u\|\nabla e_u^{n+1}\|^2+D_v\|\nabla e_v^{n+1}\|^2\\
&\le \frac{1}{2D_u}\|\varepsilon_u^{n+1}\|_*^2+\frac{1}{2D_v}\|\varepsilon_v^{n+1}\|_*^2+\frac{1}{2}(D_u+5L)\|e_u^{n+1}\|^2+\frac{D_u}{2}\|\nabla e_u^{n+1}\|^2\\
&\quad+\frac{1}{2}(D_v+9L)\|e_v^{n+1}\|^2+\frac{D_v}{2}\|\nabla e_v^{n+1}\|^2+L\left(\|e_u^n\|^2+\|e_v^n\|^2+(\|v(t_{n+1})-v(t_n)\|+\|v^n-v^{n_1}\|)^2\right).
\end{aligned}$$

Simplifying and multiplying by $2\Delta t$ yields

$$\begin{aligned}
&\|e_u^{n+1}\|^2-\|e_u^n\|^2+\|e_u^{n+1}-e_u^n\|^2+\|e_v^{n+1}\|^2-\|e_v^n\|^2+\|e_v^{n+1}-e_v^n\|^2+\Delta tD_u\|\nabla e_u^{n+1}\|^2+\Delta tD_v\|\nabla e_v^{n+1}\|^2\\
&\le \frac{\Delta t}{D_u}\|\varepsilon_u^{n+1}\|_*^2+\frac{\Delta t}{D_v}\|\varepsilon_v^{n+1}\|_*^2+\Delta t(D_u+5L)\|e_u^{n+1}\|^2+\Delta t(D_v+9L)\|e_v^{n+1}\|^2\\
&\quad+2\Delta tL\left(\|e_u^n\|^2+\|e_v^n\|^2+(\|v(t_{n+1})-v(t_n)\|+\|v^n-v^{n_1}\|)^2\right).
\end{aligned}$$

Summing for $n=0,\dots,N-1$, yields

$$\begin{aligned}
&\|e_u^N\|^2+\|e_v^N\|^2+\sum_{n=0}^{N-1}\left(\|e_u^{n+1}-e_u^n\|^2+\|e_v^{n+1}-e_v^n\|^2\right)+\Delta t\sum_{n=0}^{N-1}\left(D_u\|\nabla e_u^{n+1}\|^2+D_v\|\nabla e_v^{n+1}\|^2\right)\\
&\le (1+2\Delta tL)\left(\|e_u^0\|^2+\|e_v^0\|^2\right)+\Delta t\sum_{n=0}^{N-1}\left(\frac{1}{D_u}\|\varepsilon_u^{n+1}\|_*^2+\frac{1}{D_v}\|\varepsilon_v^{n+1}\|_*^2\right)\\
&\quad+\Delta t/\Delta t_\circ\sum_{n=0}^{N-1}\left(\|e_u^{n+1}\|^2+\|e_v^{n+1}\|^2\right)+2\Delta tL\sum_{n=0}^{N-1}(\|v(t_{n+1})-v(t_n)\|+\|v^n-v^{n_1}\|)^2.
\end{aligned}$$

Using the discrete Grönwall lemma leads to

$$\begin{aligned}
&\|e_u^N\|^2 + \|e_v^N\|^2 + \frac{1}{1-\Delta t/\Delta t_\circ}\sum_{n=0}^{N-1}\left(\|e_u^{n+1}-e_u^n\|^2 + \|e_v^{n+1}-e_v^n\|^2\right)\\
&\quad + \frac{\Delta t}{1-\Delta t/\Delta t_\circ}\sum_{n=0}^{N-1}\left(D_u\|\nabla e_u^{n+1}\|^2 + D_v\|\nabla e_v^{n+1}\|^2\right)\\
&\le \frac{1}{1-\Delta t/\Delta t_\circ}\Bigg[\left(1+2\Delta tL-\Delta t/\Delta t_\circ\right)\left(\|e_u^0\|^2+\|e_v^0\|^2\right) + \Delta t\sum_{n=0}^{N-1}\left(\frac{1}{D_u}\|\varepsilon_u^{n+1}\|_*^2 + \frac{1}{D_v}\|\varepsilon_v^{n+1}\|_*^2\right)\\
&\quad + 2\Delta tL\sum_{n=0}^{N-1}\left(\|v(t_{n+1})-v(t_n)\| + \|v^n-v^{n_1}\|\right)^2\Bigg]\exp\left(\frac{N\Delta t}{\Delta t_\circ-\Delta t}\right).
\end{aligned} \tag{2.19}$$

The expression

$$\|v(t_{n+1})-v(t_n)\| \le \Delta t^{\frac{1}{2}}\left(\int_{t_n}^{t_{n+1}}\left\|\frac{dv}{ds}(s)\right\|^2 ds\right)^{\frac{1}{2}},$$

implies

$$\sum_{n=0}^{N-1}\|v(t_{n+1})-v(t_n)\|^2 \le \Delta t\int_{t_0}^{t_N}\left\|\frac{dv}{ds}(s)\right\|^2 ds. \tag{2.20}$$

With the assumptions (2.10), (1.5), and using (2.13), we also have

$$\|v^{n_1}-v^n\| = \Delta t\|g(u^n, v^{n_1})\| \le C_g\Delta t\|v^{n_1}\| \le \frac{C_g\Delta t}{(1-2\Delta tC_g)^{\frac{1}{2}}}\|v^n\|,$$

and with (2.11) this implies

$$\sum_{n=0}^{N-1}\|v^{n_1}-v^n\|^2 \le \frac{C_g\Delta t}{2}\|v_0\|^2\exp\left(\frac{2N\Delta tC_g}{1-\Delta tC_g}\right). \tag{2.21}$$

Substituting (2.20)–(2.21) into (2.19) and using (2.14) implies

$$\begin{aligned}
&\|e_u^N\|^2 + \|e_v^N\|^2 + \frac{1}{1-\Delta t/\Delta t_\circ}\sum_{n=0}^{N-1}\left(\|e_u^{n+1}-e_u^n\|^2 + \|e_v^{n+1}-e_v^n\|^2\right)\\
&\quad + \frac{\Delta t}{1-\Delta t/\Delta t_\circ}\sum_{n=0}^{N-1}\left(D_u\|\nabla e_u^{n+1}\|^2 + D_v\|\nabla e_v^{n+1}\|^2\right)\\
&\le \frac{1}{1-\Delta t/\Delta t_\circ}\Bigg[\left(1+2\Delta tL-\Delta t/\Delta t_\circ\right)\left(\|e_u^0\|^2+\|e_v^0\|^2\right)\\
&\quad + \Delta t\sum_{n=0}^{N-1}\left(\frac{1}{D_u}\|\varepsilon_u^{n+1}\|_*^2 + \frac{1}{D_v}\|\varepsilon_v^{n+1}\|_*^2\right) + 4\Delta t^2L\int_{t_0}^{t_N}\left\|\frac{dv}{dt}(t)\right\|^2 dt\\
&\quad + 2\Delta t^2LC_g\|v_0\|^2\exp\left(\frac{2N\Delta tC_g}{1-2\Delta tC_g}\right)\Bigg]\exp\left(\frac{N\Delta t}{\Delta t_\circ-\Delta t}\right),
\end{aligned}$$

which implies (2.18). ■

Combining Lemmas 2.1 and 2.2 we derive the following error estimate that implies convergence and first-order accuracy in time for the solution u^n, v^n of (2.8a)–(2.8c), with the assumption that e_u^0, e_v^0 are also of order Δt.

Theorem 2.3. *Under the assumptions of Lemmas 2.1 and 2.2, there exists a constant $C(u, v) > 0$ such that*

$$\max_{0\le n\le N}\left(\|e_u^n\| + \|e_v^n\|\right) + \left(\Delta t\sum_{n=0}^{N-1}\left(D_u\|\nabla e_u^{n+1}\|^2 + D_v\|\nabla e_v^{n+1}\|^2\right)\right)^{\frac{1}{2}} \le C(u, v)\left(\|e_u^0\| + \|e_v^0\| + \Delta t\right).$$

Proof. Indeed,

$$\begin{aligned}
&\|e_u^N\|^2 + \|e_v^N\|^2 + \frac{\Delta t}{1-\Delta t/\Delta t_\circ}\sum_{n=0}^{N-1}\left(D_u\|\nabla e_u^{n+1}\|^2 + D_v\|\nabla e_v^{n+1}\|^2\right)\\
&\le \frac{1}{1-\Delta t/\Delta t_\circ}\Bigg[(1+2\Delta tL-\Delta t/\Delta t_\circ)\left(\|e_u^0\|^2+\|e_v^0\|^2\right)\\
&\quad+\Delta t\sum_{n=0}^{N-1}\left(\frac{1}{D_u}\|\varepsilon_u^{n+1}\|_*^2+\frac{1}{D_v}\|\varepsilon_v^{n+1}\|_*^2\right)+4\Delta t^2L\left\|\frac{dv}{dt}\right\|^2_{L^2(0,T;L^2(\Omega))}\\
&\quad+2\Delta t^2LC_g\|v^0\|^2\exp\left(\frac{2C_gN\Delta t}{1-2\Delta tC_g}\right)\Bigg]\exp\left(\frac{N\Delta t}{\Delta t_\circ-\Delta t}\right)\\
&\le \frac{1}{1-\Delta t/\Delta t_\circ}\Bigg[(1+2\Delta tL-\Delta t/\Delta t_\circ)\left(\|e_u^0\|^2+\|e_v^0\|^2\right)+\Delta t^2\int_{t_0}^{t_N}\frac{1}{D_u}\left(\left\|\frac{d^2u}{dt^2}(t)\right\|_*+L\left\|\frac{du}{dt}(t)\right\|_*\right)^2\\
&\quad+\frac{1}{D_v}\left(\left\|\frac{d^2v}{dt^2}(t)\right\|_*+L\left\|\frac{dv}{dt}(t)\right\|_*\right)^2dt+4\Delta t^2L\left\|\frac{dv}{dt}\right\|^2_{L^2(0,T;L^2(\Omega))}\\
&\quad+2\Delta t^2LC_g\|v^0\|^2\exp\left(\frac{2C_gN\Delta t}{1-2\Delta tC_g}\right)\Bigg]\exp\left(\frac{N\Delta t}{\Delta t_\circ-\Delta t}\right). \quad \blacksquare
\end{aligned}$$

3. A fully-discrete approximation

As previously pointed out, no analysis of the fully discrete problem is undertaken; nevertheless in this section the fully discrete approximations are used to generate the numerical solutions. For the numerical implementation of the IMSP scheme we employ a Galerkin finite element approximation with continuous piecewise linear basis functions as in Garvie and Trenchea [10].

For simplicity we assume that Ω is a polygonal domain. Let $\mathcal{T}^h$ be a quasi-uniform partitioning of Ω into disjoint open simplices $\{\tau\}$ with $h_\tau := \text{diam}\tau$ and $h := \max_{\tau\in\mathcal{T}^h} h_\tau$, so that $\bar{\Omega} = \cup_{\tau\in\mathcal{T}^h}\bar{\tau}$. We introduce S^h, the standard finite element space:

$$S^h := \{v \in C(\bar{\Omega}) : v|_\tau \text{ is linear } \forall\tau \in \mathcal{T}^h\} \subset H^1(\Omega).$$

We shall also need the Lagrange interpolation operator $\pi^h : C(\bar{\Omega}) \to S^h$ such that $\pi^h(v(x_j)) = v(x_j)$ for $j = 0,\dots,M$, where $\{x_j\}_{j=0}^M$ is the set of nodes of the triangulation. Let $\{\phi_j\}_{j=0}^M$ be the standard basis for S^h, satisfying $\phi_j(x_i) = \delta_{ij}$. A discrete L^2 inner product on $C(\bar{\Omega})$ is then defined by

$$(u,v)^h := \int_\Omega \pi^h(u(x)v(x))dx \equiv \sum_{j=0}^M \widehat{M}_{jj}u(x_j)v(x_j),$$

where $\widehat{M}_{jj} := (1,\phi_j) \equiv (\phi_j,\phi_j)^h > 0$, corresponding to the (diagonal) lumped Mass Matrix $\widehat{M}$. We also define $K_{ij} := (\nabla\phi_i,\nabla\phi_j)$ corresponding to the Stiffness Matrix K, and $L_{ij} := (\widehat{M}_{ii})^{-1}K_{ij}$, corresponding to the matrix $L = (\widehat{M})^{-1}K$. We denote the identity matrix to be I.

The fully-discrete finite element first-order IMSP approximation is then formulated as follows.

For $n = 0,\dots,N-1$ find $U_h^{n_1}, V_h^{n_1}, U_h^{n+1}, V_h^{n+1} \in S^h$ such that $(U_h^0, V_h^0) = (\pi^h u_0, \pi^h v_0)$ and for all $\chi_h \in S^h$

$$\left(\frac{U_h^{n+1}-U_h^{n_1}}{\Delta t},\chi_h\right)^h + D_u(\nabla U_h^{n+1},\nabla\chi_h) = 0, \tag{3.22a}$$

$$\left(\frac{V_h^{n+1}-V_h^{n_1}}{\Delta t},\chi_h\right)^h + D_v(\nabla V_h^{n+1},\nabla\chi_h) = 0, \tag{3.22b}$$

$$\left(\frac{U_h^{n_1}-U_h^{n}}{\Delta t},\chi_h\right)^h = \left(f(U_h^n,V_h^{n_1}),\chi_h\right)^h, \tag{3.22c}$$

$$\left(\frac{V_h^{n_1}-V_h^{n}}{\Delta t},\chi_h\right)^h = \left(g(U_h^n,V_h^{n_1}),\chi_h\right)^h. \tag{3.22d}$$

The Galerkin method involves choosing $U_h^n = \sum_{j=0}^M U_j^n\phi_j$, $V_h^n = \sum_{j=0}^M V_j^n\phi_j$, $\chi_h = \phi_i, i = 0,\dots,M$, where $U_j^n \approx u(x_j,t_n)$, $V_j^n \approx v(x_j,t_n)$.

After defining $\{\mathbf{U}^n\}_i = U_i^n$, $\{\mathbf{V}^n\}_i = V_i^n$, this leads to a nonlinear algebraic system that is solved via the following steps:

1. Solve the nonlinear system for the vector $\mathbf{V}^{n_1}$:

$$\mathbf{V}^{n_1} - \Delta t g(\mathbf{U}^n, \mathbf{V}^{n_1}) = \mathbf{V}^n \tag{3.23a}$$

2. Evaluate the entries of the vector $\mathbf{U}^{n_1}$:

$$\mathbf{U}^{n_1} = \mathbf{U}^n + \Delta t f(\mathbf{U}^n, \mathbf{V}^{n_1}) \tag{3.23b}$$

3. Solve the linear systems for $\mathbf{U}^{n+1}$ and $\mathbf{V}^{n+1}$:

$$(I - \Delta t D_u L)\mathbf{U}^{n+1} = \mathbf{U}^{n_1}, \tag{3.23c}$$

$$(I - \Delta t D_v L)\mathbf{V}^{n+1} = \mathbf{V}^{n_1}. \tag{3.23d}$$

Let us compare the previous scheme with the classical IMEX scheme (see e.g. formula (1.8) in Koto [23] or Scheme 2 in Garvie [11]) defined as follows:

1. Evaluate the entries of the vector $\mathbf{V}^{n_1}$:

$$\mathbf{V}^{n_1} = \mathbf{V}^n + \Delta t g(\mathbf{U}^n, \mathbf{V}^n) \tag{3.24a}$$

2. Evaluate the entries of the vector $\mathbf{U}^{n_1}$:

$$\mathbf{U}^{n_1} = \mathbf{U}^n + \Delta t f(\mathbf{U}^n, \mathbf{V}^n) \tag{3.24b}$$

3. Solve the linear systems (3.23c) and (3.23d) for $\mathbf{U}^{n+1}$ and $\mathbf{V}^{n+1}$.

The only difference between these two schemes is in the calculation of $\mathbf{V}^{n_1}$. In the IMSP scheme we must solve a nonlinear system (step (3.23a)), while for the IMEX scheme we evaluate step (3.24a). However, whenever $g(u, v) = v\tilde{g}(u)$ for a given $\tilde{g}(u)$, then (3.23a) can be replaced by the following diagonal linear system, which can be solved elementwise:

$$(I - \Delta t \mathrm{diag}(\tilde{g}(\mathbf{U}^n)))\mathbf{V}^{n_1} = \mathbf{V}^n.$$

The coefficient matrices of the linear systems (3.23c) and (3.23d) are strictly (row) diagonally dominant matrices with all off-diagonal elements negative or zero. Consequently, $(I - \Delta t D_u L)$ and $(I - \Delta t D_v L)$ are M-matrices, which guarantee that their inverses are positive. Direct solvers based on Gaussian elimination (without partial pivoting and with only one application of LU factorization) can be successfully applied. Furthermore, because of the diagonal dominance of the coefficient matrices, the GMRES algorithm with restarts may also be applied since it converges for any restart value [24,25].

4. Numerical examples

Spatially extended predator–prey models that couple logistic prey growth with Holling type II or type IV functional responses of the predators satisfy our assumptions, and are interesting from both an ecological and numerical perspective [6]. A well-known model with logistic prey growth and Holling type II functional response of the predators is the spatially explicit Rosenzweig–MacArthur (RM) model [7], and is arguably the most widely studied spatially extended predator–prey model.

In Diele et al. [13] IMSP schemes were applied to a two-dimensional phytoplankton–zooplankton RM model [26] and results compared with those from the application of a standard first-order IMEX scheme (see 'Scheme 2 with Kinetics (i)' in Garvie [11]). The IMSP schemes converged faster than the IMEX schemes, particularly during the onset of spatiotemporal chaos.

4.1. A one-dimensional example

We compare the performance of the IMSP scheme with the performance of an IMEX scheme, for the numerical solution of system (1.1a)–(1.1d) in one space dimension, where the kinetics take the following specific Holling Type II form

$$f(u, v) = u(1 - u) - v(1 - e^{-\gamma u}), \tag{4.25a}$$

$$g(u, v) = \beta v(\alpha - 1 - \alpha e^{-\gamma u}), \tag{4.25b}$$

with $\alpha, \beta, \gamma > 0$ (see Garvie and Trenchea [10]). The assumption (1.5) is satisfied with $C_g = \beta(\alpha - 1)$, as

$$g(u, v) = \beta v(\alpha - 1 - \alpha e^{-\gamma u}) \le C_g v.$$

The parameters were chosen in order to guarantee a stable limit cycle in the reaction kinetics surrounding an unstable steady state. The diffusion coefficients D_u and D_v were both set to 1 and we chose $\alpha = 1.5$, $\beta = 1$ and $\gamma = 5$. Thus, the densities of predators and prey are oscillatory, which is the situation of primary interest from an ecological point of view. The initial densities for prey and predator populations were prescribed everywhere on the domain $\Omega = [0, 1]$ to be

$u_0 = 0.2$ and $v_0 = 0.0328$ respectively, leading to spatially homogeneous solutions. A uniform grid was employed with nodes $x_j = jh, j = 0, \ldots, M, M = 1/h$, and a spatial step size $h = 1/1024$. We used the time steps $\Delta t_i = 1/2^{i+1}$ for $i = 1, \ldots, 10$. With the above choice of parameters we have $C_g = 0.5$, and so for stability of the IMSP scheme (see (2.10)) it is sufficient to take $\Delta t < 1$.

As no exact solution is known, the spatially homogeneous finite element solutions were compared with the numerical solution of the ODE system

$$\frac{dU}{dt} = D_u LU + U(1-U) - V(1-e^{-\gamma U}), \tag{4.26a}$$

$$\frac{dV}{dt} = D_v LV + \beta V(\alpha - 1 - \alpha e^{-\gamma U}), \tag{4.26b}$$

computed using `ode15s` in Matlab, with absolute and relative tolerance set to 10^{-15} and 10^{-13} respectively. For notational convenience we denote the solution vector for the ODE approximations of the prey density at $T = 20$ to be $\widetilde{\mathbf{U}}$, where $\{\widetilde{\mathbf{U}}\}_j = \widetilde{U} \approx U(20)$, for $j = 0, \ldots, 1024$.

The errors in the prey densities were calculated via

$$E_i^{(U)} = \|\widetilde{\mathbf{U}} - \mathbf{U}^{N_i}\| = \max_{0\le j\le M} |\widetilde{U} - U_j^{N_i}|,$$

and plotted in Fig. 1(a) with respect to Δt_i for $i = 1, \ldots, 10$ using logarithmic scales for both axes. The slopes of the convergence curves are both equal to 1, confirming the first-order rate of convergence in time of the IMEX and IMSP schemes. The numerical results also show that the errors for the IMSP scheme are on the order of 10^{-1} less than the errors for the IMEX scheme, confirming the superior accuracy of the IMSP scheme. Similar results were obtained for predator densities (results omitted).

In Fig. 1(b) we plot predator densities against prey densities at $x = 1/2$ in the time interval $[170, 200]$. Using the same value of the time step ($\Delta t = 0.1$), the limit cycle computed with the IMSP scheme is closer to the 'theoretical' limit cycle computed with `ode15s` than the limit cycle computed with the IMEX scheme. Logarithmic scales were used for both axes for a better display of the differences between the curves. The numerical approximations for the IMSP scheme were computed using the Matlab code `fd1dKin2IMSP`, which is freely available at http://www.uoguelph.ca/~mgarvie/.

4.2. A two-dimensional example

We compare the performance of the IMSP scheme with the performance of an IMEX scheme, for the numerical solution of system (1.1a)–(1.1d) in two space dimension, where the kinetics take the following specific Rosenzweig–MacArthur form

$$f(u,v) = u(1-u) - \frac{uv}{u+\alpha}, \tag{4.27a}$$

$$g(u,v) = \frac{\beta uv}{u+\alpha} - \gamma v, \tag{4.27b}$$

with $\alpha, \beta, \gamma > 0$ (see Garvie and Trenchea [10] and Medvinsky et al. [26]). The assumption (1.5) is satisfied with $C_g = |\beta - \gamma|$, as

$$g(u,v) = \frac{\beta uv}{u+\alpha} - \gamma v = \left(\frac{\beta u}{u+\alpha} - \gamma\right) v \le C_g v.$$

We repeat a numerical experiment undertaken in Garvie et al. [27], where the domain models a hypothetical lake with an island, and the unstructured mesh was generated by the Matlab program `Mesh2d v2.3`.[1] The mesh is a triangularization of $M = 427$ nodes (Fig. 2(a)). As in the one dimensional examples, the parameters were chosen to ensure oscillatory reaction kinetics, namely: $D_u = D_v = 1, \alpha = 0.4, \beta = 0.2$ and $\gamma = 0.6$. The spatially heterogeneous initial data was prescribed as[2]:

$$u_0(x,y,0) = 6/35 - 2\times 10^{-7}(x - 0.1y - 225)(x - 0.1y - 675),$$

$$v_0(x,y,0) = 116/245 - 3\times 10^{-5}(x - 450) - 1.2\times 10^{-4}(y - 150).$$

The reaction–diffusion system was approximated with different time steps and comparisons made between the performance of the IMEX and IMSP schemes. With the above choice of parameters we have $C_g = 0.4$, and so for stability of the IMSP scheme (see (2.10)) it is sufficient to take $\Delta t < 0.8$.

In the first set of experiments we compare accuracy and rates of convergence of the ISMP and the IMEX schemes. As no exact solution is known, in place of a theoretical solution several candidate solutions are considered when estimating

[1] Freely available at https://www.mathworks.com/matlabcentral/fileexchange/.

[2] Parameter values and data are given in `fe2dnfasttest`, downloadable from the above mentioned webpage.

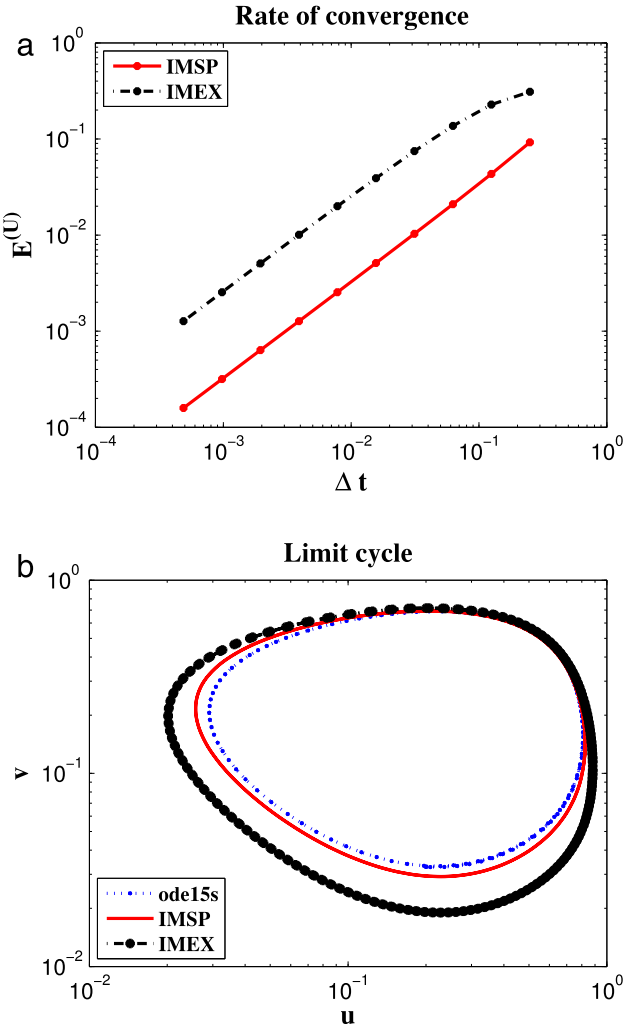

Fig. 1. (a): Convergence rates and accuracy comparisons between the IMEX and IMSP schemes at $T = 20$. The two curves have the same slope, thus confirming the same order of convergence, however, the IMSP solutions are clearly more accurate than the IMEX solutions. (b): limit cycle curves for the evolution of the predator–prey population in the time interval [170, 200] at the point $x = 1/2$. The limit cycle computed using the IMSP scheme is closer to the 'theoretical' limit cycle evaluated with `ode15s` than the limit cycle computed with the IMEX scheme.

the errors. We refer to these candidate solutions as 'reference solutions'. For the first reference solution the continuous in time solutions were solved with the Matlab code `ode15s`, with absolute and relative tolerance set to 10^{-15} and 10^{-13}. As with the IMEX and IMSP schemes, the reaction–diffusion system is approximated in space using the standard Galerkin finite element method. However, for the temporal discretization the resulting 427 coupled ODEs were solved using `ode15s`. The remaining two reference solutions were computed using the IMEX and IMSP schemes with a fine temporal grid $\Delta t = 1/2^{10}$, and are denoted `IMEXfine` and `IMSPfine` respectively.

The solution vectors for the approximations to the IMEX and IMSP schemes are both denoted $\mathbf{U}^{N_i}$ and $\mathbf{V}^{N_i}$, for $n = 0, 1, \ldots, N_i - 1$ with $N_i = 50/\Delta t_i$ and $\Delta t_i = 1/2^i$ for $i = 1, \ldots, 6$. For notational convenience we denote the solution vector for all three reference solutions of prey density at $T = 50$ to be $\widetilde{\mathbf{U}}$, where $\{\widetilde{\mathbf{U}}\}_j = \widetilde{U}_j \approx u(x_j, 50)$, for $j = 0, \ldots, 427$.

The errors in the prey densities were calculated via

$$E_i^{(U)} = \|\widetilde{\mathbf{U}} - \mathbf{U}^{N_i}\| = \max_{0 \le j \le 427} |\widetilde{U}_j - U_j^{N_i}|,$$

and plotted in Fig. 2(b) with respect to Δt_i for $i = 1, \ldots, 6$, using logarithmic scales for both axes. The numerical results are consistent with the first-order rate of convergence of both IMEX and IMSP schemes. Furthermore, the error curves for the IMSP scheme lie below the error curves for the IMEX scheme, for all three reference solutions, confirming the superior accuracy of the IMSP scheme. Similar results were obtained for predator densities (results omitted).

Finally, we show in Fig. 3 the finite element approximations of prey densities on the two-dimensional lake domain at $T = 150$ using the IMEX and IMSP schemes. The left column of Fig. 3 displays the numerical approximations for the IMSP

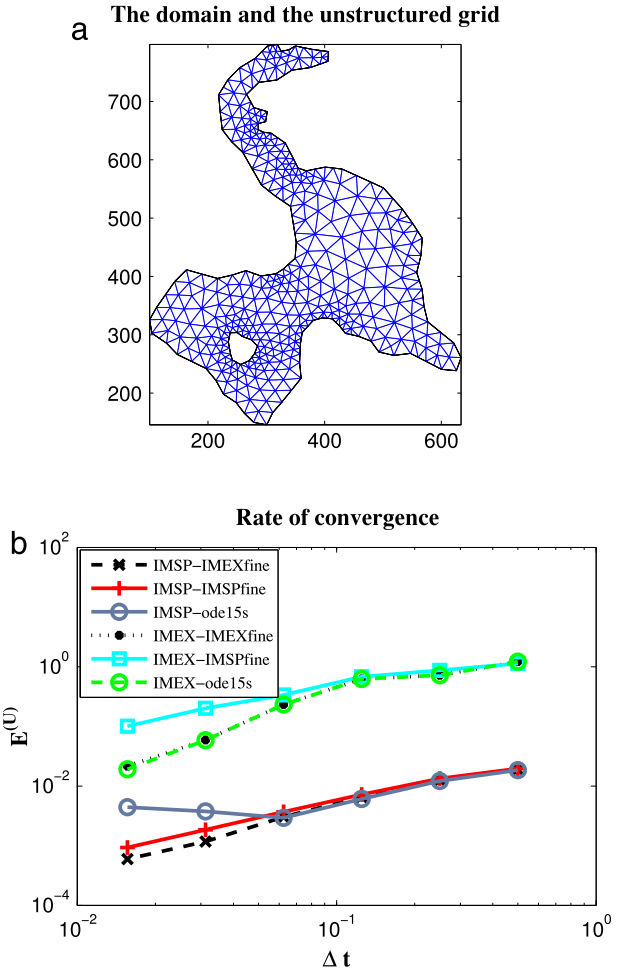

Fig. 2. (a): A hypothetical lake domain with an island and the grid with 427 nodes (see Garvie et al. [27]). (b): convergence rates for the IMEX and IMSP schemes. For each scheme the rate of convergence has been evaluated with respect to three different reference solutions: `ode15s`, IMEXfine and IMSPfine. See the text for further details.

scheme with successively smaller time steps, namely: $\Delta t = 1/3$ (Fig. 3(a)), $\Delta t = 1/24$ (Fig. 3(c)), and $\Delta t = 1/384$ (Fig. 3(e)). The right column of Fig. 3 displays the numerical approximations for the IMEX scheme with a corresponding reduction in time steps. The numerical results seem to suggest that the IMSP scheme is more accurate than the IMEX scheme.

The first-order IMEX scheme was implemented using the Matlab code `fe2dnfast`. We also modified the time-stepping procedure for the IMEX scheme to generate the Matlab code `fe2dnfastIMSP`, which implements the first-order IMSP scheme.[3]

5. Conclusion

We performed the rigorous numerical analysis of the semi-discrete in time approximations of a first-order implicit-symplectic (IMSP) scheme for reaction–diffusion systems modelling predator–prey dynamics. The IMSP scheme is a novel method that effectively approximated the oscillatory dynamics due to a centre-type equilibrium (see Settanni and Sgura [16]). In this paper we focused our analysis on a specific class of reaction kinetics based on logistic prey growth and 'Holling type' functional response [6] of the predators. This is the case of the well-known Rosenzweig–MacArthur model [7].

We derived semi-discrete *a priori* bounds on the time step which guaranteed positive and stable solutions. Moreover, we proved an optimal *a priori* error estimate for the semi-discrete solutions of the IMSP scheme. Results from numerical experiments in one and two space dimensions seem to suggest that the IMSP scheme is more accurate than a standard first-order implicit–explicit (IMEX) scheme for approximating two well-known spatially extended predator–prey models.

Future research could focus on the numerical analysis of the associated fully-discrete problem, by mimicking the semi-discrete estimates in the fully-discrete case (see e.g. Garvie and Trenchea [10]). However, the numerical analysis

[3] Both codes are freely available at http://www.uoguelph.ca/~mgarvie/.

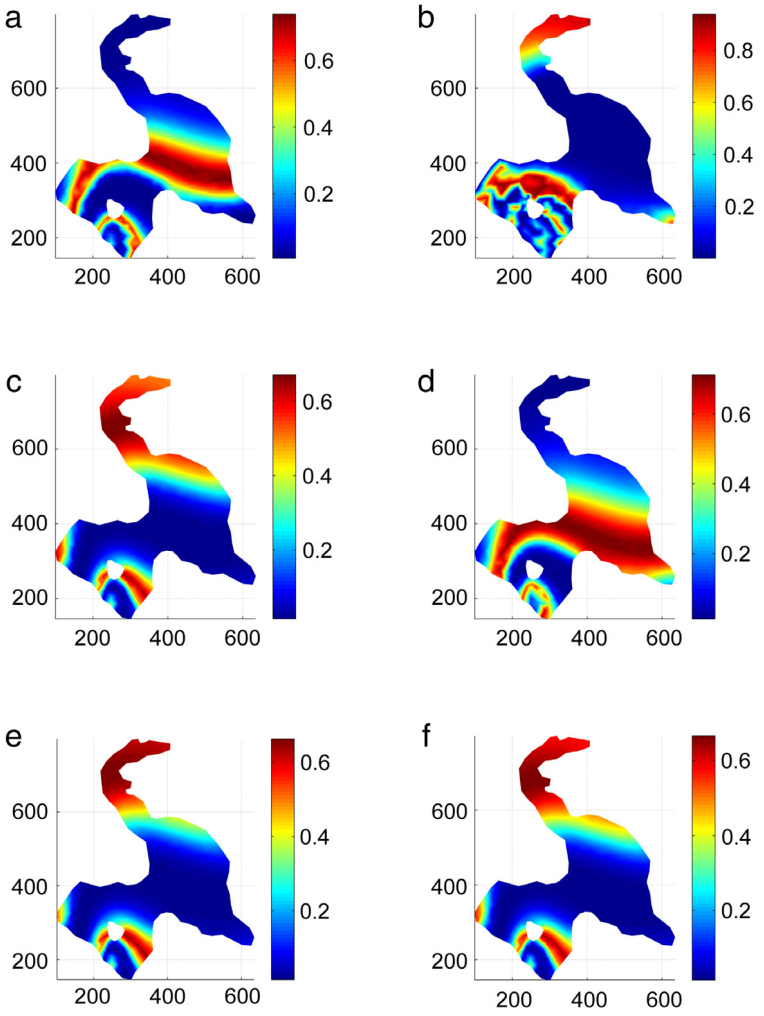

Fig. 3. Two dimensional finite element prey approximations of system (1.1a)–(1.1d) with kinetics (4.27a)–(4.27b) at $T = 150$ using the IMSP scheme (left column figures) and the IMEX scheme (right column figures). Plots show successive time step refinement: (a)–(b) $\Delta t = 1/3$, (c)–(d) $\Delta t = 1/24$, (e)–(f) $\Delta t = 1/384$. See the text for the parameter values and initial data.

of the corresponding fully-discrete IMSP problem is tedious and requires additional standard techniques from the finite element method for elliptic problems, e.g. interpolation error estimates, inverse estimates, and error estimates for numerical integration [28]. Furthermore, the analysis of the fully-discrete schemes would yield no additional information about the superiority of IMSP scheme with respect to IMEX scheme, since the advantage of the IMSP methods is due to the time stepping procedure.

A more promising area of future research is the analysis of the semi-discrete in time formulation of a second-order implicit-symplectic (IMSP) scheme [13], which is currently in progress.

Acknowledgements

This work has been carried out within the H2020 project 'ECOPOTENTIAL: Improving Future Ecosystem Benefits Through Earth Observations', coordinated by CNR-IGG (http://www.ecopotential-project.eu). The project has received funding from the European Union's Horizon 2020 research and innovation programme under grant agreement No. 641762 (F. Diele). This work was partially supported by NSERC Discovery Grant #400159 (M. Garvie), and partially supported by the AFOSR under grant FA 9550-12-1-0191, and by NSF grant DMS-1522574 (C. Trenchea).

References

[1] R.S. Cantrell, C. Cosner, Spatial Ecology via Reaction–diffusion Equations, in: Wiley Series in Mathematical and Computational Biology, John Wiley & Sons, Ltd., Chichester, 2003, URL http://dx.doi.org/10.1002/0470871296.

[2] M.R. Garvie, C. Trenchea, Spatiotemporal dynamics of two generic predator–prey models, J. Biol. Dyn. 4 (6) (2010) 559–570. URL http://dx.doi.org/10.1080/17513750903484321.
[3] W. Gentleman, A. Leising, B. Frost, S. Strom, J. Murray, Functional responses for zooplankton feeding on multiple resources: a review of assumptions and biological dynamics, Deep-Sea Res. II 50 (2003) 2847–2875.
[4] J.M. Jeschke, M. Kopp, R. Tollrian, Predator functional responses: Discriminating between handling and digesting prey, Ecol. Monogr. 72 (1) (2002) 95–112. URL http://www.jstor.org/stable/3100087.
[5] G.T. Skalski, J.F. Gilliam, Functional responses with predator interference: Viable alternatives to the Holling type II model, Ecology 82 (2001) 3083–3092.
[6] C.S. Holling, Some characteristics of simple types of predation and parasitism, Can. Entomol. 91 (1959) 385–398. URL http://journals.cambridge.org/article-S0008347X00072692.
[7] M.L. Rosenzweig, R.H. MacArthur, Graphical representation and stability conditions of predator–prey interactions, Am. Nat. 97 (895) (1963) 209–223. URL http://www.jstor.org/stable/2458702.
[8] J. Sherratt, M. Lewis, A. Fowler, Ecological chaos in the wake of invasion, Proc. Natl. Acad. Sci. 92 (1995) 2524–2528.
[9] E. Hansen, F. Kramer, A. Ostermann, A second-order positivity preserving scheme for semilinear parabolic problems, Appl. Numer. Math. 62 (10) (2012) 1428–1435. URL http://dx.doi.org.pitt.idm.oclc.org/10.1016/j.apnum.2012.06.003.
[10] M.R. Garvie, C. Trenchea, Finite element approximation of spatially extended predator–prey interactions with the Holling type II functional response, Numer. Math. 107 (4) (2007) 641–667. URL http://dx.doi.org/10.1007/s00211-007-0106-x.
[11] M.R. Garvie, Finite-difference schemes for reaction–diffusion equations modeling predator–prey interactions in MATLAB, Bull. Math. Biol. 69 (3) (2007) 931–956. URL http://dx.doi.org/10.1007/s11538-006-9062-3.
[12] E. Hairer, C. Lubich, G. Wanner, Geometric Numerical Integration, in: Springer Series in Computational Mathematics, vol. 31, Springer, Heidelberg, 2010, Structure-preserving algorithms for ordinary differential equations, Reprint of the second (2006) edition.
[13] F. Diele, C. Marangi, S. Ragni, IMSP schemes for spatially explicit models of cyclic populations and metapopulation dynamics, Math. Comput. Simulation 100 (2014) 41–53. URL http://dx.doi.org/10.1016/j.matcom.2014.01.006.
[14] F. Diele, C. Marangi, S. Ragni, Implicit-symplectic partitioned (IMSP) Runge–Kutta schemes for predator–prey dynamics, AIP Conf. Proc. 1479 (1) (2012) 1177–1180. URL http://scitation.aip.org/content/aip/proceeding/aipcp/10.1063/1.4756360.
[15] M. Beck, M. Gander, On the positivity of Poisson integrators for the Lotka–Volterra equations, BIT 55 (2) (2015) 240–319.
[16] G. Settanni, I. Sgura, Devising efficient numerical methods for oscillating patterns in reaction–diffusion systems, J. Comput. Appl. Math. 292 (2016) 674–693. URL http://dx.doi.org.pitt.idm.oclc.org/10.1016/j.cam.2015.04.044.
[17] J. Guckenheimer, P. Holmes, Nonlinear Oscillations, Dynamical Systems, and Bifurcations of Vector Fields, in: Applied Mathematical Sciences, vol. 42, Springer-Verlag, New York, 1990, revised and corrected reprint of the 1983 original.
[18] V. Barbu, Partial Differential Equations and Boundary Value Problems, in: Mathematics and its Applications, vol. 441, Kluwer Academic Publishers, Dordrecht, 1998, translated and revised from the 1993 Romanian original by the author.
[19] L. Evans, Partial Differential Equations, in: Graduate Studies in Mathematics, vol. 19, American Mathematical Society, Providence, RI, 1998.
[20] E. DiBenedetto, Partial Differential Equations, second ed., in: Cornerstones, Birkhäuser Boston, Inc., Boston, MA, 2010, URL http://dx.doi.org/10.1007/978-0-8176-4552-6.
[21] M.R. Garvie, Analysis of a reaction–diffusion system of $\lambda - \omega$ type (Ph.D. thesis), University of Durham, 2003.
[22] M.R. Garvie, C. Trenchea, A three level finite element approximation of a pattern formation model in developmental biology, Numer. Math. 127 (3) (2014) 397–422. URL http://dx.doi.org.pitt.idm.oclc.org/10.1007/s00211-013-0591-z.
[23] T. Koto, IMEX Runge-Kutta schemes for reaction–diffusion equations, J. Comput. Appl. Math. 215 (1) (2008) 182–195. URL http://dx.doi.org.pitt.idm.oclc.org/10.1016/j.cam.2007.04.003.
[24] Y. Saad, M.H. Schultz, GMRES: a generalized minimal residual algorithm for solving nonsymmetric linear systems, SIAM J. Sci. Stat. Comput. 7 (3) (1986) 856–869. URL http://dx.doi.org/10.1137/0907058.
[25] Y. Saad, Iterative Methods for Sparse Linear Systems, second ed., Society for Industrial and Applied Mathematics, Philadelphia, PA, 2003, URL http://dx.doi.org/10.1137/1.9780898718003.
[26] A.B. Medvinsky, S.V. Petrovskii, I.A. Tikhonova, H. Malchow, B.-L. Li, Spatiotemporal complexity of plankton and fish dynamics, SIAM Rev. 44 (3) (2002) 311–370. electronic. URL http://dx.doi.org/10.1137/S0036144502404442.
[27] M.R. Garvie, J. Burkardt, J. Morgan, Simple finite element methods for approximating predator–prey dynamics in two dimensions using Matlab, Bull. Math. Biol. 77 (3) (2015) 548–578. URL http://dx.doi.org/10.1007/s11538-015-0062-z.
[28] P.G. Ciarlet, The Finite Element Method for Elliptic Problems, in: Studies in Mathematics and its Applications, vol. 4, North-Holland Publishing Co., Amsterdam, 1978.